High-efficient phosphorescent iridium(III) complexes with benzimidazole ligand for organic light-emitting diodes: Synthesis, electrochemistry and electroluminescent properties

Chunxiang Li [a], Guanghui Zhang [b], Hung-Hsin Shih [d], Xiaoqing Jiang [b], Peipei Sun [b,*], Yi Pan [c,*], Chien-Hong Cheng [d]

[a] College of Chemistry and Molecular Engineering, Qingdao University of Science and Technology, Qingdao 266042, PR China
[b] Jiangsu Key Laboratory of Biofunctional Materials, College of Chemistry and Environmental Science, Nanjing Normal University, 122, Ninghai Road, Nanjing, Jiangsu 210097, PR China
[c] School of Chemistry and Chemical Engineering, Nanjing University, Nanjing 210093, PR China
[d] Department of Chemistry, Tsing Hua University, Hsinchu 300, Taiwan

ARTICLE INFO

ABSTRACT

Two phosphorescent complexes Ir(FFBI)$_2$(pmp) and Ir(FFBI)$_2$(pti) based on cyclometalated ligand 1-(4-fluorobenzyl)-2-(4-fluorophenyl)-1H-benzo[d]imidazole (FFBI) and ancillary ligands 2-(phenyliminom-ethyl)phenol (pmp) or 3-(pyridin-2-yl)-4,5,6,7-tetrahydro-2H-indazole (pti) were synthesized. The single crystal of Ir(FFBI)$_2$(pmp) was obtained. The light emitting and electrochemical properties of these complexes were studied. The electroluminescent devices based on these two complexes with the structure of ITO/NPB (40 nm)/Ir complex: CBP (30 nm)/BCP (15 nm)/Alq (30 nm)/LiF (1 nm)/Al (100 nm) emitted cyan color, with high brightness and efficiencies. The maximum external quantum efficiencies reached to 6.8% and 11.6%, respectively.

1. Introduction

Electrophosphorescent materials incorporating complexes of heavy metals have been aroused particularly attention in last decade due to their extremely high efficiency as electroluminescent emitters. They mainly include square planar d^8 or octahedral d^6 complexes of heavy-metals such as Pt(II), Ru(II), Os(II), and Ir(III) [1–6]. Of these materials, iridium complexes have been regarded as the most appropriate phosphorescent materials because of their relatively short lifetime and high quantum efficiency. These Ir complexes generally contain two cyclometalated ligands (ĈN) and a single bidentate, monoanionic ancillary ligand, or with three cyclometalated ligands. The cyclometalated ligands used in the complexes are well known as heterocycle derivatives that coordinated to the metal center *via* formation of Ir–N and Ir–C bonds. Therefore, design of ligands for Ir complexes is of great importance in order to achieve high efficiency and color purity for OLEDs. To date, most researches were focused on the design and synthesis of the cyclometalated ligand, such as changing π conjugation, introducing electron donating or withdrawing group on the appropriate position of the aromatic ring [7–10], and adopting rigid structure, as

we recently reported [11], to get high efficient and full-color emitting materials, while the study to the ancillary ligand was deficient though it was shown that the ancillary ligand has an evident effect on the properties of materials [12–14]. And also, a majority of complexes obtained by modifying cyclometalated ligand emit green or red color, while blue-emitting iridium complexes, which are important for the realization of RGB full-color displays and the creation of white light-emitting devices (WOLEDs), are still scarce. In our previous report, a complex Ir(FFBI)$_2$(acac) with green emitting and high efficiencies was studied [15]. In this work, using 1-(4-fluorobenzyl)-2-(4-fluorophenyl)-1H-benzo[d]imidazole (FFBI) as cyclometalated ligand, by introducing two novel ancillary ligands, two new complexes were synthesized. They showed obvious blue shift compared to Ir(FFBI)$_2$(acac). The devices based on these two complexes gave high brightness and external quantum efficiencies.

2. Results and discussion

2.1. Synthesis and structural characterization of the complexes

Scheme 1 shows the synthetic procedure for the ligands and the corresponding iridium complexes. The cyclometalated ligand 1-(4-fluorobenzyl)-2-(4-fluorophenyl)-1H-benzo[d]imidazole (FFBI)

* Corresponding authors. Tel./fax: +86 25 83598280 (P.P. Sun).
E-mail address: sunpeipei@njnu.edu.cn (P.P. Sun).
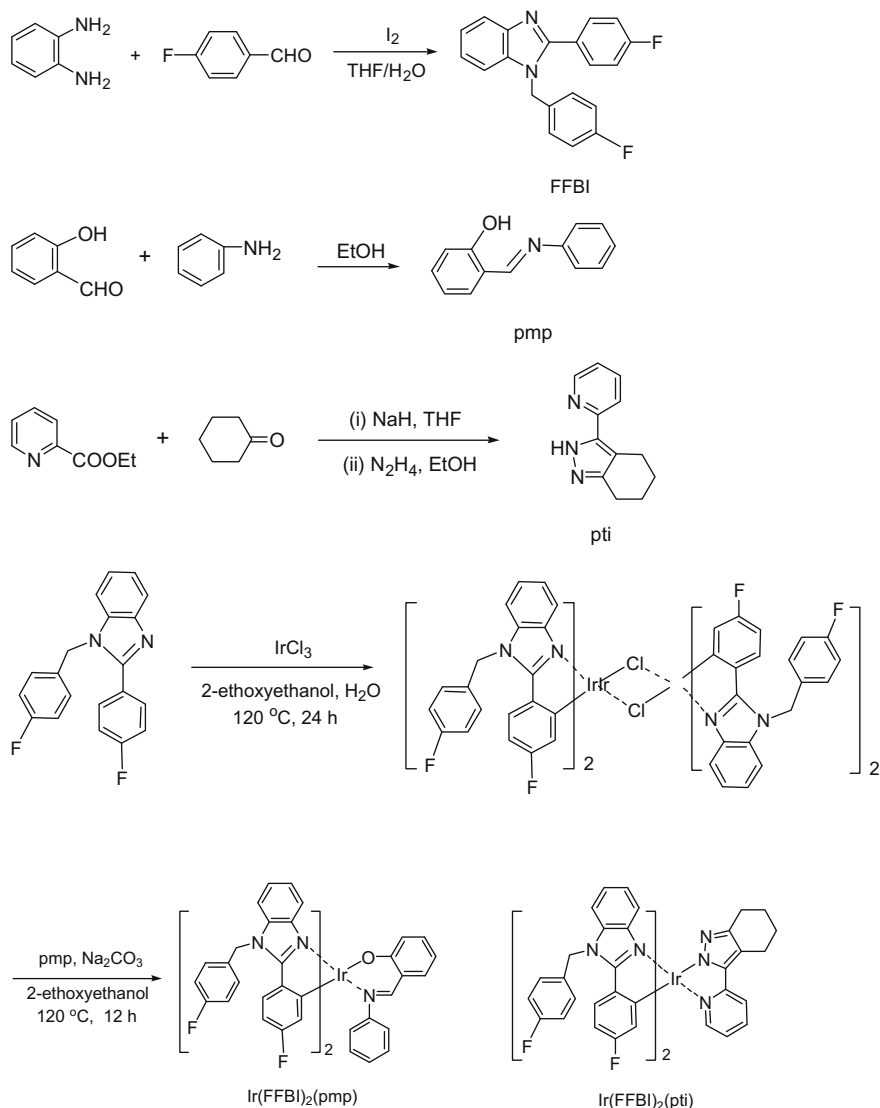
Scheme 1. Synthesis of the iridium complexes.

was conveniently prepared by the reaction of 1,2-phenylenedi-amine and 4-fluorobenzaldehyde catalyzed by iodine [16]. The ancillary ligand 2-(phenyliminomethyl)phenol (pmp) was easily achieved by the condensation of salicylaldehyde with aniline. The ligand 3-(pyridin-2-yl)-4,5,6,7-tetrahydro-2H-indazole (pti) was synthesized by the condensation of ethyl picolinate and cyclohex-anone, followed by treatment with hydrazine hydrate in refluxing ethanol [17]. The complexes were synthesized by a general proce-dure [18]. The reaction of iridium trichloride hydrate with cylco-metalated ligands FFBI gave the Ir(III) μ-chlorobridged dimer. Then the dimer reacted with ancillary ligand pmp or pti in the presence of base to afford the desired iridium complexes Ir(FF-BI)$_2$(pmp) and Ir(FFBI)$_2$(pti) in moderate yields. The complexes were purified by column chromatography then sublimated at 300–320 °C and 4×10^{-3} Pa. Their structures were characterized by ^{1}H NMR, IR, mass spectra and elemental analyses.

X-ray crystallographic studies have been carried out for Ir(FF-BI)$_2$(pmp). The crystal structure and crystal packing diagram of Ir(FFBI)$_2$(pmp) are shown in Figs. 1 and 2. Selected bond distances and bond angles are listed in Table 1. The complex exhibits slightly distorted octahedral coordination geometry around Ir atom with the cis-O, N, cis-C, C, and trans-N, N chelate disposition. The angles

of trans ligands at the metal center range between 171.2 and 179.4° and the bond lengths range between 2.005 and 2.147 Å. The atoms are nearly planar with the torsion angles of N4–N1–N2–C46 2.69 (0.11)°, O1–N2–C26–N4 3.88 (0.13)°, and O1–N1–C26–C46 2.12 (0.15)°. The two phenyl groups of pmp are perpen-dicular each other with dihedral angle of 90.09°.

2.2. Electrochemical properties

In order to investigate the highest occupied molecular orbital (HOMO) and the lowest unoccupied molecular orbital (LUMO) en-ergy levels of the two complexes, cyclic voltammetry was carried out. On the basis of the onset potential of the oxidation, HOMO en-ergy level of the two Ir complexes can be estimated with regard to the energy level of the ferrocenium/ferrocene redox couple (being approximately 4.8 eV negative to the vacuum level) [19].

The HOMO energy level of Ir(FFBI)$_2$(pti) was calculated to be −5.04 eV which is very close to that of Ir(FFBI)$_2$(pmp). This is con-sistent with the reported electrochemical studies and theoretical calculations that the one-electron oxidation of such d^6 complexes would mainly occur at the metal site, together with a minor contri-bution from the surrounding chelates [12,20].
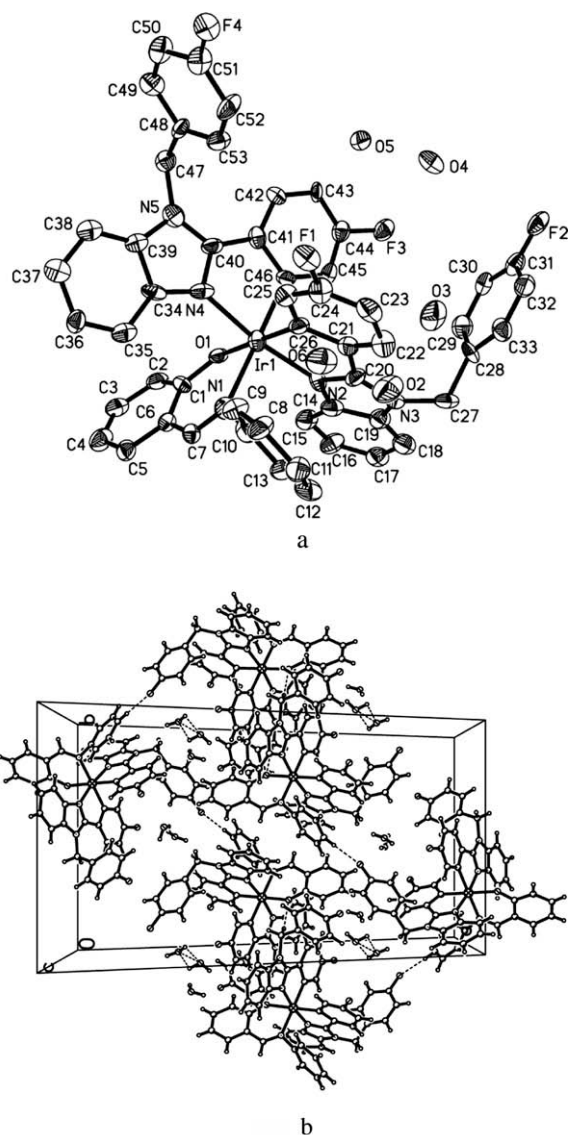
Fig. 1. (a) Molecular structure of Ir(FFBI)$_2$(pmp) with thermal ellipsoids drawn at the 30% probability level. (b) Packing diagram viewed from the *c*-axis. The broken lines show intermolecular hydrogen bonding.
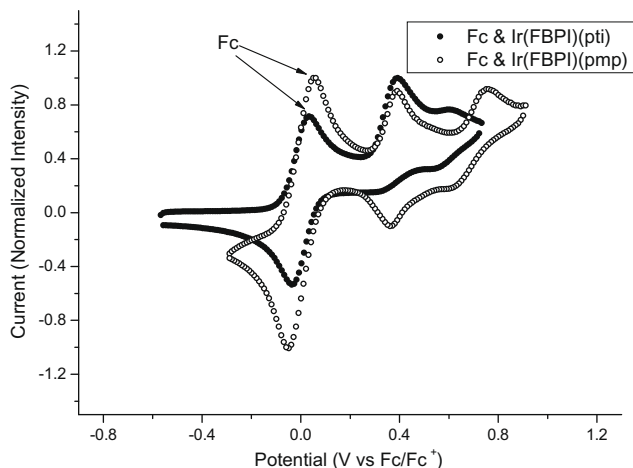
Table 1
The selected bond lengths (Å), angles (°).

Bond distance (Å)			
Ir(1)–O(1)	2.138(4)	Ir(1)–C(46)	2.073(5)
Ir(1)–N(1)	2.147(5)	F(1)–C(24)	1.404(7)
Ir(1)–N(2)	2.052(5)	F(2)–C(31)	1.349(8)
Ir(1)–N(4)	2.071(4)	F(3)–C(44)	1.438(8)
Ir(1)–C(26)	2.005(6)	F(4)–C(51)	1.337(4)
Bond angle (°)			
O(1)–Ir(1)–N(1)	86.42(15)	N(1)–Ir(1)–C(46)	179.4(2)
O(1)–Ir(1)–N(2)	96.83(15)	N(2)–Ir(1)–N(4)	171.21(18)
O(1)–Ir(1)–N(4)	87.73(16)	N(2)–Ir(1)–C(26)	81.0(2)
O(1)–Ir(1)–C(26)	177.2(2)	N(2)–Ir(1)–C(46)	93.1(2)
O(1)–Ir(1)–C(46)	93.28(19)	N(4)–Ir(1)–C(26)	94.2(2)
N(1)–Ir(1)–N(2)	87.54(19)	N(4)–Ir(1)–C(46)	79.1(2)
N(1)–Ir(1)–N(4)	100.29(18)	C(26)–Ir(1)–C(46)	85.1(2)
N(1)–Ir(1)–C(26)	95.3(2)	Ir(1)–O(1)–C(1)	128.3(3)

Table 2
The electrochemical behavior of Ir(FFBI)$_2$(pmp) and Ir(FFBI)$_2$(pti).

Complex	E_{onset} (V)	$E_{1/2}$ (V)	λ (nm)[a]	E_g (eV)[b]	HOMO (eV)[c]	LUMO (eV)[d]
Ir(FFBI)$_2$(pti)	0.24	0.37	444	2.79	−5.04	−2.25
Ir(FFBI)$_2$(pmp)	0.27	0.38	461	2.69	−5.07	−2.38

[a] Obtained from the wavelength at the intersection of absorption and emission spectra.
[b] $E_g = hc/\lambda = 1241/\lambda$ (nm).
[c] Calculated from onset oxidation potential.
[d] Calculated from E_g and HOMO energy level.

From the HOMO energy level and the energy gap calculated from the wavelength at the intersection of UV–Vis absorption and emission spectra, the LUMO energy level can be estimated [21] (Table 2). For the two complexes, Ir(FFBI)$_2$(pti) has a greater energy gap so a blue shift of the PL spectrum was observed.

2.3. Absorption and emission

Fig. 3 depicts the UV–Vis and photoluminescence (PL) spectra of Ir(FFBI)$_2$(pmp) and Ir(FFBI)$_2$(pti) in dichloromethane at room temperature. For Ir(FFBI)$_2$(pmp), there are three major absorptions at 299, 377, and 431 nm in the UV–Vis spectrum. The former intense absorption band appears to be ligand-based transition that closely resembles the spectrum of the free ligand FFBI, whereas the latter two absorptions are likely due to ^{1}MLCT and ^{3}MLCT according to
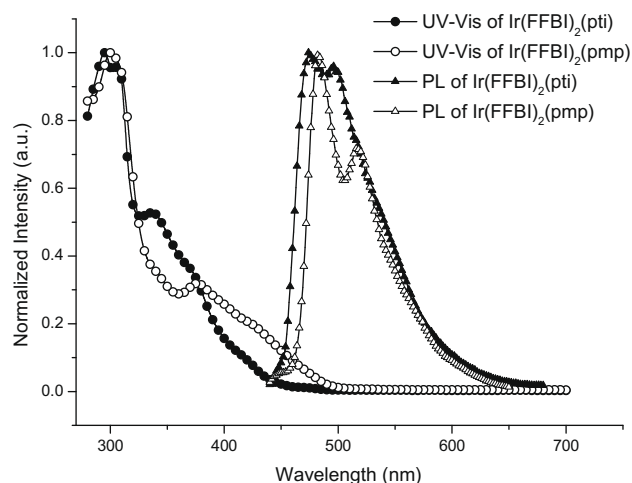

Fig. 2. The cyclic voltammograms of Ir(FFBI)$_2$(pmp) and Ir(FFBI)$_2$(pti).

Fig. 3. The UV–Vis absorption and photoluminescence spectra of the iridium complexes Ir(FFBI)$_2$(pmp) and Ir(FFBI)$_2$(pti) in CH$_2$Cl$_2$.

the previous reports and the calculations of Hay [20]. Similar result was observed for complex Ir(FFBI)$_2$(pti). For many luminescent organic molecules, the absorption spectrum overlaps on the emission spectrum, especially for heavy metal complexes due to their metal to ligand charge transfer (MLCT) [11]. Based on the wavelengths at which the UV–Vis absorption and photoluminescent spectra intersect, the energy gap between LUMO and HOMO can be calculated.

On irradiation with 340 nm light, both Ir(FFBI)$_2$(pmp) and Ir(FFBI)$_2$(pti) showed strong photoluminescence in dichloromethane at 483 and 474 nm, respectively, falling in blue to cyan region. Compared to Ir(FFBI)$_2$(acac) [15], Ir(FFBI)$_2$(pmp) and Ir(FFBI)$_2$(pti) exhibits 10 and 20 nm blue shift of emission maximum, respectively. The results indicated that besides the cyclometalated ligand, ancillary ligand also has an obvious effect on changing the emitting wavelength. Through selecting appropriate ancillary ligand to get diverse color emitting complexes, especially blue-emitting iridium complexes will be possible.

2.4. Electroluminescent properties

To illustrate the electroluminescent properties of these complexes, typical OLED devices (device A and B) using complex Ir(FFBI)$_2$(pmp) and Ir(FFBI)$_2$(pti) respectively as dopants were fabricated. The devices had a multi-layer configuration ITO/NPB (40 nm)/Ir complex: CBP (30 nm)/BCP (15 nm)/Alq (30 nm)/LiF (1 nm)/Al (100 nm), in which ITO (indium tin oxide) was used as the anode, NPB (4,4′-bis[N-(1-naphthyl)-N-phenylamino]biphenyl) was used as the hole-transporting material, CBP (4,4′-N,N′-dicarbozole biphenyl) as the host, the iridium complexes as the dopant, BCP (2,9-dimethyl-4,7-dipheny-1,10-phenanthroline) as the hole blocker, Alq (tris(8-hydroxyquinolinato)aluminium) as the electron transporter, and LiF/Al as the cathode (Fig. 4). Key characteristics of these devices are listed in Table 3.
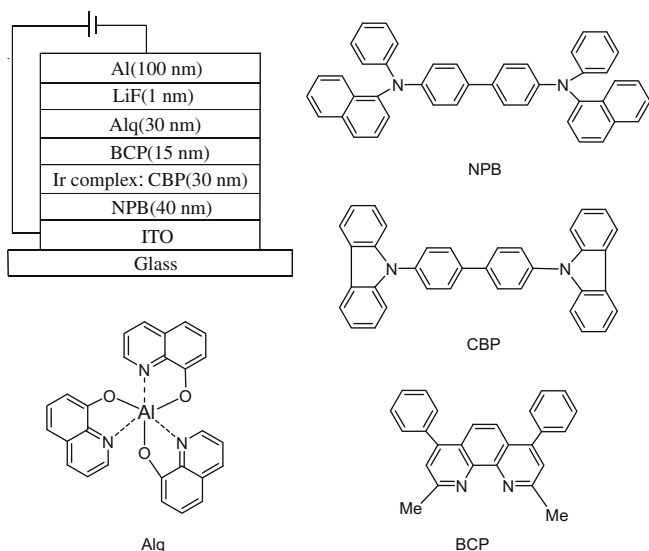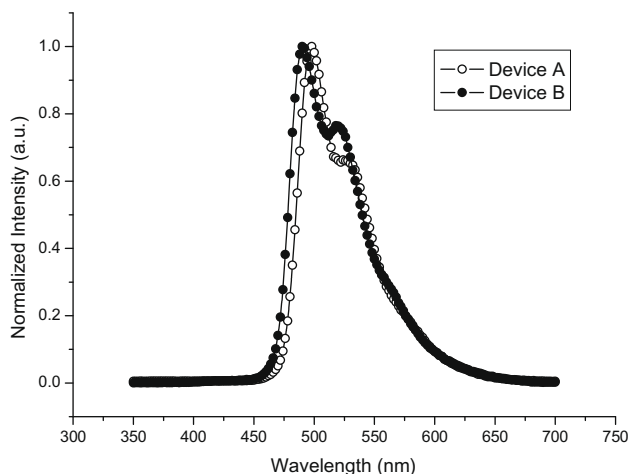

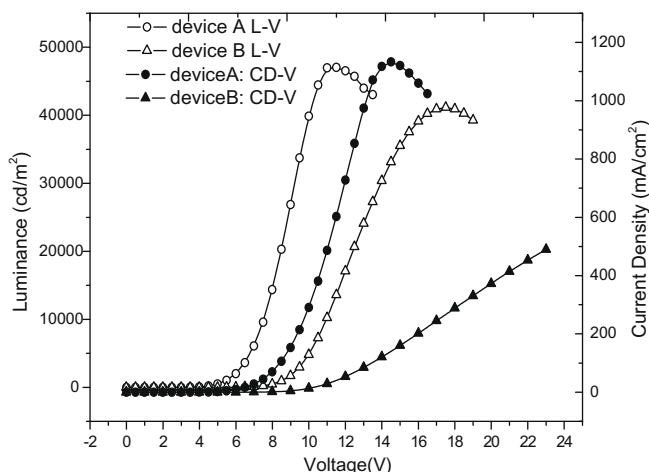**Fig. 5.** The electroluminescence spectra of devices.

Fig. 6. The luminance–voltage–current (L–V–I) characteristics of the devices.

Device A and B emitted strong cyan light with an emission maximum at 498, 492 nm, respectively (Fig. 5). It is surprising to note that compared to the PL spectra of Ir(FFBI)$_2$(pmp) and Ir(FFBI)$_2$(pti) in dichloromethane solution, the maximum emission wavelength and the shape of the electroluminescence spectra are substantially different, the maximum emission wavelength of device B exhibited a red shift up to 18 nm. Though the certain reason for the difference is not yet clear, we can presume that the different environment in dichloromethane solution and in thin film had different effect on the emission of the complex. The EL spectra of devices do not change significantly with variation of the applied voltages from 6 to 12 V. Based on the EL spectrum at an applied voltage of 8 V, The Commission International de I'Eclairage (CIE) coordinates of device A and B are (0.23, 0.58), (0.22, 0.54), respectively. The CIE coordinate of both complexes are almost independent of driving voltage.

Fig. 4. The general structure of devices and the molecular structures of the compounds used in the devices.

Table 3
The performance data of the Ir complex-based OLEDs.

Device	Turn-on voltage (V)	η_{ext} (%, V)	L (cd/m², V)	η_c (cd/A, V)	η_p (lm/W, V)	λ_{max} (nm)	CIE, 8 V (x, y)
A: 7.3%Ir(FFBI)$_2$(pmp)	3.4	6.8, 6.5	47100, 11.5	21.7, 6.5	15.4, 4.0	498	(0.23, 0.58)
B: 6.7%Ir(FFBI)$_2$(pti)	3.1	11.6, 9.0	41150, 17.5	35.3, 9.0	14.8, 4.9	492	(0.22, 0.54)

The data for external quantum efficiency (η_{ext}), brightness (L), current efficiency (η_c), and power efficiency (η_p) are the maximum values of the devices.
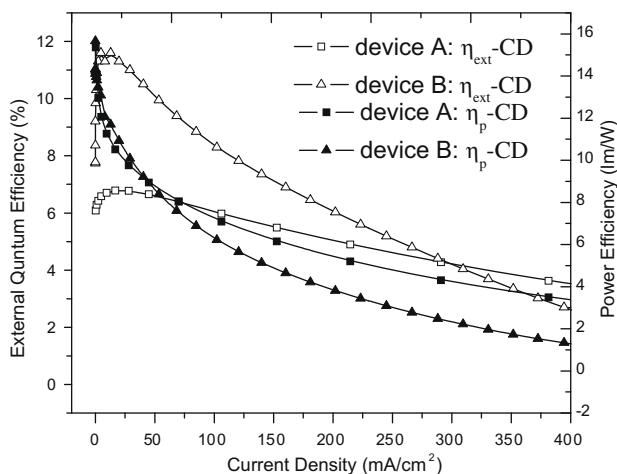
Fig. 7. The external quantum efficiency (η_{ext})–current density–power efficiency (η_p) characteristics of the devices.

Figs. 6 and 7 show the luminance–voltage–current (L–V–I) and the external quantum efficiency (η_{ext})–current density–power efficiency (η_p) characteristics of the devices, respectively. Both devices showed quite high efficiencies and brightness. Device A, with 7.3% of Ir(FFBI)$_2$(pmp), appears to show the better performance in terms of brightness and power efficiency, with brightness of 47 100 cd/m^2 at 11.5 V and 15.4 lm/W at 3.5 V. For device B, with 6.7% of Ir(FFBI)$_2$(pti) as dopant, an extremely high external quantum efficiency of 11.6%, a maximum brightness of 41 150 cd/m^2 at 17.5 V, and a current efficiency of 35.3 cd/A were achieved (Table 3).

Another attractive feature of device A is the slow decay of external quantum efficiency with increasing current density, as shown in Fig. 6. The device gave a peak external quantum efficiency η_{ext} of 6.8% at $J = 16.62$ mA/cm^2. When the current density increased to $J = 100$ mA/cm^2, the external quantum efficiency η_{ext} decreased to 6.08% with a loss of about 10%. At $J = 200$ mA/cm^2, the value of η_{ext} still remained as high as 5.06%.

3. Conclusion

In summary, we synthesized two iridium complexes Ir(FFBI)$_2$(pmp) and Ir(FFBI)$_2$(pti) by used a cyclometalated ligand FFBI with two novel ancillary ligands pmp and pti. The EL devices based on these two iridium complexes emitted cyan color, with high brightness and efficiencies. Designing novel ancillary ligands is shown to be a direction to get high efficient diverse color emitting electrophosphorescent complexes.

4. Experimental

4.1. Reagents and instruments

Reagents were used as purchased without further purification. ^{1}H NMR spectra were measured on a Bruker ARX-400 spectrometer in CDCl$_3$ using TMS as an internal reference. Mass spectra (MS) were measured on a VG-ZAB-HS spectrometer with electron impact ionization. Elemental analysis was performed on a Perkin–Elmer 240C elemental analyzer. The UV–Vis spectra were recorded on a VARIAN Cary 5000 spectrometer. PL spectra were recorded on a Perkin–Elmer LS 50B luminescence spectrophotometer. Cyclic voltammetry (CV) measurements were carried out with a CHI660C electrochemical analyzer (CH Instruments) at room temperature using 0.10 M tetra(n-butyl)ammonium hexafluorophosphate

(TBAP) as the supporting electrolyte and degassed dichloromethane as the solvent. The ferrocenium/ferrocene couple was used as the internal standard. Current, voltage, and light-intensity measurements were made simultaneously using a Keithley 2400 source meter and a Newport 1835-C optical meter equipped with a Newport 818-ST silicon photodiode.

4.2. Preparation of ligands

4.2.1. 1-(4-Fluorobenzyl)-2-(4-fluorophenyl)-1H- benzo[d]imidazole (FFBI)

1,2-Phenylenediamine (0.54 g, 5 mmol) and 4-fluorobenzaldehyde (1.06 g, 10 mmol) were dissolved in THF–H$_2$O (v/v 1:1, 20 mL), and then iodine (0.03 g, 0.1 mmol) was added. After stirred for 3 h at room temperature, the mixture was extracted with CH$_2$Cl$_2$, the solution was evaporated and the residue was then purified by column chromatography over silica gel using petroleum ether/ethyl acetate (v/v, 4:1) as eluent to furnish pure FFBI in 72% yield. M.p. 88–90 °C. ^{1}H NMR (CDCl$_3$, 400 MHz) δ: 8.13–8.16 (m, 1H), 7.88 (d, $J = 7.4$ Hz, 1H), 7.64–7.68 (m, 2H), 7.28–7.32 (m, 3H), 7.13–7.16 (m, 2H), 7.05–7.09 (m, 3H), 5.43 (s, 2H). MS (EI) m/z: 320.1 (51.9, M$^+$), 228.9 (7.7), 210.9 (7.3), 108.9 (100), 82.9 (19.8). Anal. Calc. for C$_{20}$H$_{14}$N$_2$F$_2$: C, 74.99; H, 4.41; N, 8.75. Found: C, 74.95; H, 4.45; N 8.71%.

4.2.2. 2-((Phenylimino)methyl)phenol (pmp)

Salicylaldehyde (1.22 g, 10 mmol) and aniline (0.93 g, 10 mmol) were dissolved in ethanol (20 mL). After stirred for 1 h at room temperature, the crystal appeared. The precipitate was filtered, recrystallized from ethanol, to give pmp in 85% yield. M.p. 50–52 °C. ^{1}H NMR (CDCl$_3$, 400 MHz) δ: 8.65 (s, 1H), 7.38–7.48 (m, 4H), 7.30–7.34 (m, 3H), 7.07 (d, $J = 8.0$ Hz, 1H), 6.97 (t, $J = 7.5$ Hz, 1H).

4.2.3. 3-(Pyridin-2-yl)-4,5,6,7-tetrahydro-2H-indazole (pti)

To a round-bottomed flask (100 mL), NaH (1.56 g, 30 mmol) and anhydrous THF (30 mL) were added. After cooled to 0 °C, the solution of cyclohexanone (2.94 g, 30 mmol) in THF (5 mL) was slowly added in it. The mixture was stirred for 30 min at room temperature, ethyl picolinate (3.85 g, 28.5 mmol) was added in dropwise at 60 °C. After refluxed for 3 h, the mixture was cooled to 0 °C, and then poured slowly into dilute hydrochloric acid. After adjusted to pH 8–9 by Na$_2$CO$_3$, the mixture was extracted with ethyl acetate, and the organic layer was washed with saturated NaCl and water. The solvent was evaporated to get brown oil.

The above obtained oil was dissolved in ethanol (90 mL), heated to boiling, 85% hydrazine hydrate (15.8 mL) was added in drops. After the mixture was refluxed for 12 h, the solvent was evaporated, and the residue was dissolved in ethyl acetate, and then washed with water. After dried with anhydrous sodium sulfate, the mixture was concentrated and then purified by column chromatography over silica gel using petroleum ether/ethyl acetate (v/v, 5:1) as eluent to give white solid pti in 55% yield. M.p. 120–121 °C. ^{1}H NMR (CDCl$_3$, 400 MHz) δ: 8.64 (d, $J = 6.5$ Hz, 1H), 7.74 (dd, $J = 7.7$, 8.0 Hz, 1H), 7.60 (d, $J = 8.0$ Hz, 1H), 7.46–7.49 (m, 1H), 2.70–2.85 (m, 4H), 1.78–1.87 (m, 4H). Anal. Calc. for C$_{12}$H$_{13}$N$_3$: C, 72.33; H, 6.58; N, 21.09. Found: C, 72.41; H, 6.52; N 20.99%.

4.3. Preparation of Ir complexes

The mixture of FFBI (0.70 g, 2.2 mmol), IrCl$_3$·3H$_2$O (0.34 g, 1 mmol) in a mixed solvent of 2-ethoxyethanol (10 mL) and water (3 mL) was stirred under N$_2$ at 120 °C for 24 h. Cooled to room temperature, the precipitate was collected by filtration and washed with water, ethanol and acetone successively, and then dried in vacuum to give a cyclometalated Ir(III) l-chloro-bridged dimer.

The dimmer, the ancillary ligand (1 mmol) and Na_2CO_3 (0.3 g) were dissolved in 2-ethoxyethanol (8 mL) and the mixture was stirred under N_2 at 120 °C for 10 h. After cooled to room temperature, the precipitate was filtered and washed with water, ethanol and acetone. The crude product was flash chromatographed on silica gel using CH_2Cl_2 as eluent to afford the desired Ir(III) complex.

Ir(FFBI)$_2$(pmp): Yield 65%.^{1}H NMR (CDCl$_3$, 400 MHz) δ: 8.07 (d, J = 7.9 Hz, 1H), 7.86 (d, J = 7.6 Hz, 1H), 7.41–7.44 (m, 2H), 7.32–7.36 (m, 4H), 7.21–7.23 (m, 2H), 7.14–7.16 (m, 3H), 7.02–7.07 (m, 7H), 6.87–6.89 (m, 3H), 6.23–6.38 (m, 5H), 6.00–6.07 (m, 2H), 5.99 (s, 2H), 5.53–5.64 (m, 4H). MS (ESI) m/z: 1027.0 (M$^+$). Anal. Calc. for $C_{53}H_{36}F_4IrN_5O$: C, 61.98; H, 3.53; N, 6.82. Found: C, 62.12; H, 3.61; N, 6.73%. IR (KBr, cm^{-1}): 2924 (w), 2344 (w), 16079 (s), 1561 (m), 1510 (m), 1463 (m), 1433 (m), 1354 (w), 1279 (w), 1254 (w), 1230 (w), 1190 (m), 1168 (w), 1125 (w), 825 (w), 697 (w).

Ir(FFBI)$_2$(pti): Yield 58%. ^{1}H NMR (CDCl$_3$, 400 MHz) δ: 7.85 (d, J = 5.4 Hz, 1H), 7.65–7.68 (m, 2H), 7.44–7.46 (m, 2H), 7.22–7.25 (m, 2H), 7.14–7.17 (m, 3H), 7.03–7.07 (m, 8H), 6.85–6.91 (m, 2H), 6.09–6.13 (m, 2H), 6.05–6.09 (m, 2H), 5.93–6.01 (m, 2H), 5.55–5.68 (m, 4H), 2.73–2.91 (m, 4H), 1.78–1.81 (m, 4H). MS (ESI) m/z: 1029.1 (M$^+$). Anal. Calc. for $C_{52}H_{38}F_4IrN_7$: C, 60.69; H, 3.72; N, 9.53. Found: C, 60.83; H, 3.58; N 9.61%. IR (KBr, cm^{-1}): 2929 (w), 2368 (w) 1602 (m), 1599 (m), 1506 (m), 1462 (s), 1279 (w), 1229 (w), 1190 (w), 1163 (w), 868 (w), 822 (w), 748 (w).

4.4. OLED fabrication

The complexes were sublimated at 300–320 °C and 4×10^{-3} Pa before use. The device was fabricated by vacuum deposition of the materials at 1.3×10^{-4} Pa onto a clean glass pre-coated with a layer of indium tin oxide with a sheet resistance of 25 $\Omega\ \square^{-1}$. The deposition rate for the organic compounds was 0.1–0.2 nm s^{-1}. The cathode of LiF/Al was deposited by first evaporating LiF at a deposition rate of 0.01 nm s^{-1} and then evaporating aluminum at a rate of 0.1–0.2 nm s^{-1}.

References

[1] M.A. Baldo, D.F. O'Brien, Y. You, A. Shoustikov, S. Sibley, M.E. Thompson, S.R. Forrest, Nature 395 (1998) 151.
[2] M.A. Baldo, M.E. Thompson, S.R. Forrest, Nature 403 (2000) 750.
[3] S. Lamansky, P. Djarovich, D. Murphy, F.A. Razzaq, R. Kwong, I. Tsyba, M. Bortz, B. Mui, R. Bau, M.E. Thompson, J. Am. Chem. Soc. 123 (2001) 4304.
[4] J.P. Duan, P.P. Sun, C.H. Cheng, Adv. Mater. 15 (2003) 224.
[5] Y.L. Tung, S.W. Lee, Y. Chi, Y.T. Tao, C.H. Chien, Y.M. Cheng, P.T. Chou, S.M. Peng, C.S. Liu, J. Mater. Chem. 15 (2005) 460.
[6] H. Xia, Y.Y. Zhu, D. Lu, M. Li, C.B. Zhang, B. Yang, Y.G. Ma, J. Phys. Chem. B 110 (2006) 18718.
[7] V.V. Grushin, N. Herron, D.D. LeCloux, W.J. Marshall, V.A. Petrov, Y. Wang, Chem. Commun. (2001) 1494.
[8] S. Okada, K. Okinaka, H. Iwawaki, M. Furugori, M. Hashimoto, T. Mukaide, J. Kamatani, S. Igawa, A. Tsuboyama, S. Takiguchi, K. Ueno, Dalton Trans. (2005) 1583.
[9] D.K. Rayabarapu, B.M.J.S. Paulose, J.P. Duan, C.H. Cheng, Adv. Mater. 17 (2005) 349.
[10] I. Avilov, P. Minoofar, J. Cornil, L.D. Cola, J. Am. Chem. Soc. 129 (2007) 8247.
[11] J.W. Hu, G.H. Zhang, H.H. Shih, X.Q. Jiang, P.P. Sun, C.H. Cheng, J. Organomet. Chem. 693 (2008) 2798.
[12] J. Li, P.I. Djurovich, B.D. Alleyne, M. Yousufuddin, N.N. Ho, J.C. Thomas, J.C. Peters, R. Bau, M.E. Thompson, Inorg. Chem. 44 (2005) 1713.
[13] L.Q. Chen, H. You, C.L. Yang, D.G. Ma, J.G. Qin, Chem. Commun. (2007) 1352.
[14] C.J. Chang, C.H. Yang, K. Chen, Y. Chi, C.F. Shu, M.L. Ho, Y.S. Yeh, P.T. Chou, Dalton Trans. (2007) 1881.
[15] C.X. Li, J.W. Hu, P.P. Sun, Y. Pan, C.H. Cheng, Chin. J. Inorg. Chem. 23 (2007) 392.
[16] P.P. Sun, Z.X. Hu, J. Heterocyclic Chem. 43 (2006) 773.
[17] P.C. Wu, J.K. Yu, Y.H. Song, Y. Chi, P.T. Chou, S.M. Peng, G.H. Lee, Organometallics 22 (2003) 4938.
[18] M. Nonoyama, Bull. Chem. Soc. Jpn. 47 (1974) 767.
[19] F.I. Wu, H.J. Su, C.F. Shu, L. Luo, W.G. Diau, C.H. Cheng, J.P. Duan, G.H. Lee, J. Mater. Chem. 15 (2005) 1035.
[20] P.J. Hay, J. Phys. Chem. A 106 (2002) 1634.
[21] J.J. Lin, W.S. Liao, H.J. Huang, F.I. Wu, C.H. Cheng, Adv. Funct. Mater. 18 (2008) 485.